Molecular and Nano-engineering with iron, ruthenium and carbon: Hybrid structures for sensing

Geest, E.P. van

Chapter 5

Monitoring a ruthenium-based photoreaction with graphene on paper

Paper-based graphene devices are appealing sensors, as the porosity of cellulose paper brings analytes in solutions close to the graphene-paper interface. We fabricated graphene field effect transistors (GFETs) on paper to sense the chemical reactions between the metal complex [Ru(tpy)(biq)(OH_2)]$^{2+}$, obtained from hydrolysis of [Ru(tpy)(biq)(Cl)]Cl, and the ligand 2-deoxyguanosine monophosphate (dGMP): in the dark, dGMP binds to ruthenium giving [Ru(tpy)(biq)(dGMP)]$^{2+}$, while it releases upon visible light irradiation. After the devices were soaked with aqueous solutions of either [Ru(tpy)(biq)Cl]Cl, the complex [Ru(bpy)$_3$]Cl_2 (which does not exchange ligands upon light irradiation), or KNO_3, they showed a strong light response: the resistance abruptly varied when the irradiation was switched on and off. When the gate potential was varied, we could observe the Dirac peak in the plots of R vs. V_{gate}, which did not shift as we switched the lamp on and off. Yet, a plot of the leak current vs. V_{gate} did show peaks indicative of electrochemistry taking place. Finally, phototriggered release of dGMP from [Ru(tpy)(biq)(dGMP)]$^{2+}$ appeared to cause a negative shift in the Dirac point, yet we could not definitively conclude that this shift is due solely to the photochemical conversion, as multiple electrochemical processes seem to contribute to the light response of the GFET. With this work, we demonstrated the power of paper in graphene devices, thus adding new concepts to the field of flexible electronics and graphene-based sensing.

E.P. van Geest, J. de Ruiter, D. van den Bos, C. Blet, J. van Ruitenbeek, G.F. Schneider and S. Bonnet, manuscript in preparation.

5.1. Introduction

Electronic devices are typically constructed on silicon wafer chips, the current industry standard.[1] Yet, these chips are brittle, as are some electronic components like the commonly used electrode indium tin oxide (ITO) for example, and both components cannot be bent or stretched.[2] For the development of flexible electronics, for instance flexible sensors, solar panels, LEDs and transistors that can for example be worn on the body, such brittle components have to be replaced.[3] 'Ordinary' paper (cellulose paper) was proposed as a good candidate to replace brittle silicon wafer substrates, because next to its abundance and flexibility, paper is a porous material, which allows solutions to be transferred inside the material through capillary forces.[4] Moreover, fluidic systems for aqueous solutions can be designed in paper substrates by simply infusing parts of the paper with a hydrophobic material, for instance wax or a photoresist, to create a (micro)fluidic system in the paper itself, which is useful for sensing technologies that probe liquid samples (*e.g.* blood or urine).[5]

Next to paper, the 2D semiconductor graphene (mono- and few layer) is an interesting candidate to be used in flexible electronics as it has shown great resilience to mechanical deformations.[6] The electronic properties of graphene are in fact very suitable for sensing.[7] For example, graphene-on-paper-based NO_2 sensors were developed, which could detect NO_2 up to 300 ppt.[8] Notably, paper-supported graphene (as large sheets or flakes) were used for example in supercapacitors, water purification devices, biomimetic devices, sensors, and energy devices.[9] These examples show the technological versatility of paper as a support for graphene, graphene oxide and reduced graphene oxide.

We wondered if we could use the sensing abilities of graphene on paper for electrical monitoring of a chemical reaction. We chose to study a photochemical reaction, using aqueous solutions of [Ru(tpy)(biq)Cl]Cl ([**1**]Cl, where tpy = 2,2';6',2''-terpyridine and biq = 2,2'-biquinoline), which is converted into $[Ru(tpy)(biq)(dGMP)]^{2+}$ ($[\mathbf{2}]^{2+}$) when a dGMP ligand (2-deoxyguanosine monophosphate) coordinates in the dark to $[Ru(tpy)(biq)(OH_2)]^{2+}$ ($[\mathbf{3}]^{2+}$). Complex $[\mathbf{3}]^{2+}$ was obtained from [**1**]Cl by hydrolysis when this complex is dissolved in chloride-free aqueous solutions.[10]. Ruthenium-purine bonds, like the Ru-dGMP bond, can be photo-labile;[11] indeed, the equilibrium between $[\mathbf{2}]^{2+}$ and $[\mathbf{3}]^{2+}$ is sensitive to light (as described in Chapter 6). Upon visible light irradiation of

complex $[\mathbf{2}]^{2+}$, the ruthenium-dGMP coordination bond is broken and dGMP is released to afford $[\mathbf{3}]^{2+}$ (see Figure 5.1A). These reactions may occur in the paper substrate, if the paper is soaked with the ruthenium-containing solution. We switched the light on and off while monitoring the resistance of the graphene sheet on top of the soaked paper (see Figure 5.1B). The aim was to study if the electrical resistance of graphene would vary upon phototriggered release of dGMP from $[\mathbf{2}]^{2+}$, as this photoreaction is expected to change the dipole moments of the reagents in solution, while graphene is sensitive to dipole changes at its surface.[7] As such, graphene on paper may be used as a sensing platform for chemical reactions in solution (see Figure 5.1B).

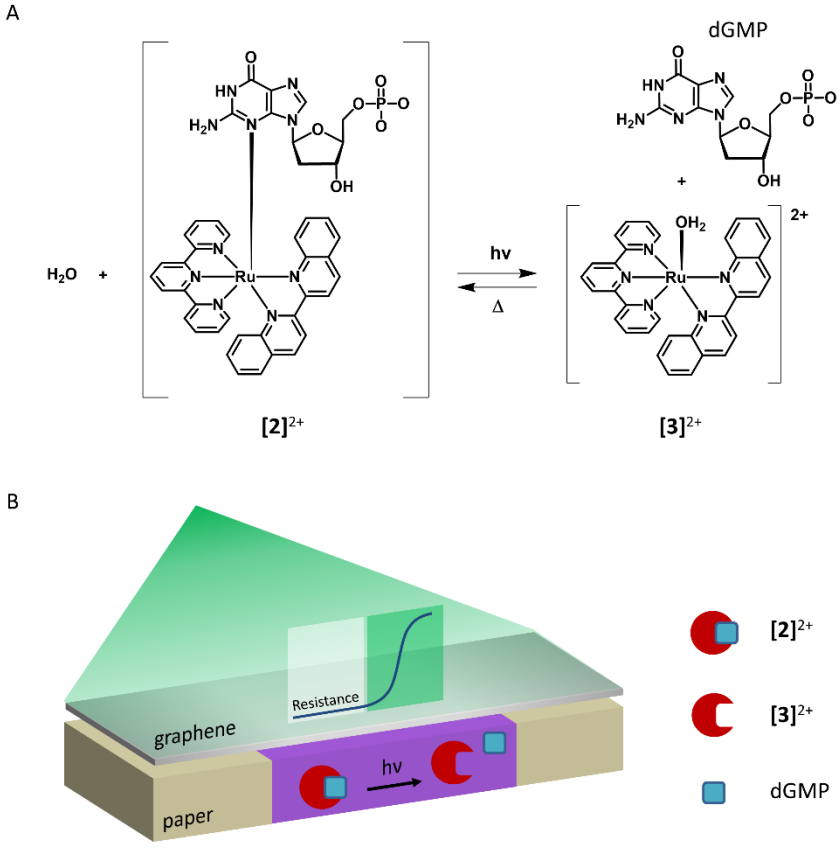

Figure 5.1: Monitoring a photochemical conversion with a GFET on paper. A) Equilibrium reaction of $[Ru(tpy)(biq)(dGMP)]^{2+}$: complex $[\mathbf{2}]^{2+}$ is stable in the dark, while green light irradiation breaks the coordination bond between Ru and dGMP, yielding free dGMP and $[Ru(tpy)(biq)(OH_2)]^{2+}$, complex $[\mathbf{3}]^{2+}$. B) Schematic representation of a graphene field effect transistor on paper for monitoring the light-sensitive equilibrium reaction between complex $[\mathbf{2}]^{2+}$ in the dark and complex $[\mathbf{3}]^{2+}$ + free dGMP upon green light irradiation.

5.2. Results and Discussion

5.2.1. Device fabrication

Graphene field-effect transistors (GFETs) on standard printing paper (Xerox, 80 g/m2, A4) were fabricated in a step-by-step fashion (see Figure 5.2). First, the paper was cut to size (2 x 3 cm, I). Then, the paper was immersed in a cellulose acetate butyrate (CAB) solution from two opposite sides to make these areas hydrophobic, leaving an untreated, hydrophilic channel in the center (II). After fixing the paper to a glass slide used as a support, the electrodes *A*, *B*, *C* and *D* were fabricated using a silver-based conductive epoxy directly on the CAB-coated areas (III). We used a four-terminal configuration for these devices: the outer electrodes *A* and *D* were used for current supply, and the inner electrodes *B* and *C* for measuring the electrical potential. Next, a sheet of PMMA-coated graphene was transferred over the electrodes (IV) and a strip of copper foil, electrically connected with a copper wire, was inserted underneath the untreated channel (V). This copper foil functioned as a gate electrode for gating experiments. The epoxy electrodes were connected to copper wires as well to finish the device (VI). For a photograph of a finished device, see Figure S5.1. Typically, the electrical resistance between electrodes *B* and *C* bordering the channel was in the range of 1-10 kΩ. A reservoir was placed in contact with the top of the paper device to ensure constant wetting of the hydrophilic channel during measurements (VII). This reservoir could be filled with a solution of interest, which soaked the untreated channel in the paper with this solution.

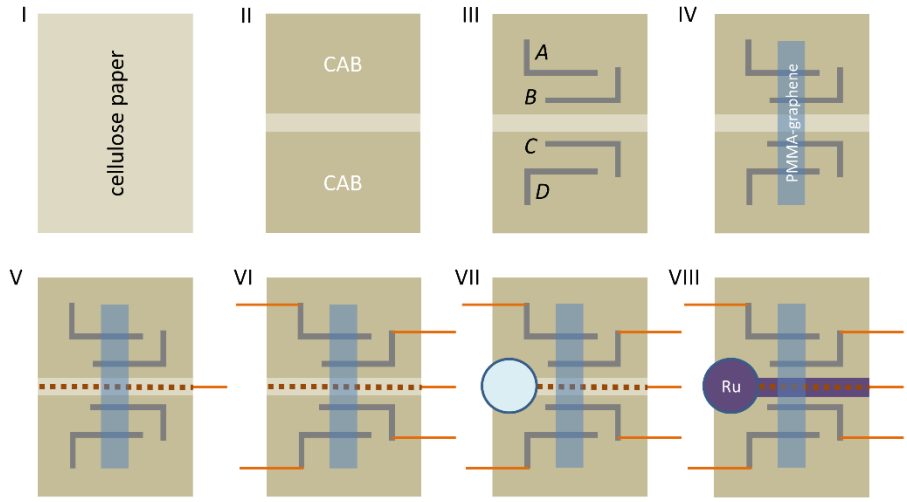

Figure 5.2: Schematic representation of the fabrication process for graphene field effect transistors on paper. First, the paper was cut to size (I), then soaked with a CAB solution, leaving a hydrophilic channel (II). Electrodes *A*, *B*, *C*, and *D* were fabricated (III), and PMMA-coated graphene was transferred on top (IV). A copper foil back gate was installed (V), and the electrodes were connected with Cu wires (VI). Finally, a reservoir was placed (VI) for wetting of the devices with the solution of interest (VIII).

5.2.2. Resistance responses to light

Finished devices were electrically connected in a closed steel box setup to shield them from electrical interference and ambient light (see Figure S5.1). On the lid of the box, a green-light LED (530 nm, P = 8.15 mW) was installed to irradiate the devices with green light, which fits with the absorption maximum of [**3**]$^{2+}$ (λ_{max} = 550 nm).[10] The devices were characterized using resistance (R) measurements *vs.* time (V_{AD} = 250 mV, see Figure 5.3A). Devices were first wetted with solutions of [**1**]Cl which hydrolyses into [**3**]$^{2+}$ (1 mM), [Ru(bpy)$_3$]Cl$_2$ ([**4**]Cl$_2$, where bpy = 2,2'dipyridine, 1 mM), or KNO$_3$ (1 mM). We used [**4**]Cl$_2$ as it is a known photocatalyst which can efficiently transfer an electron to an electron acceptor upon visible light irradiation (λ_{max} = 452 nm), [12] for instance to perform water oxidation[13] or hydrogen evolution,[14] but which cannot do photosubstitution at room temperature (Figure 5.3B). After stabilization of the soaked device in the dark for 1000 seconds, the green light intensity on the device was varied between 0 and 8.15 mW, by switching on and off the LED every 500 seconds.

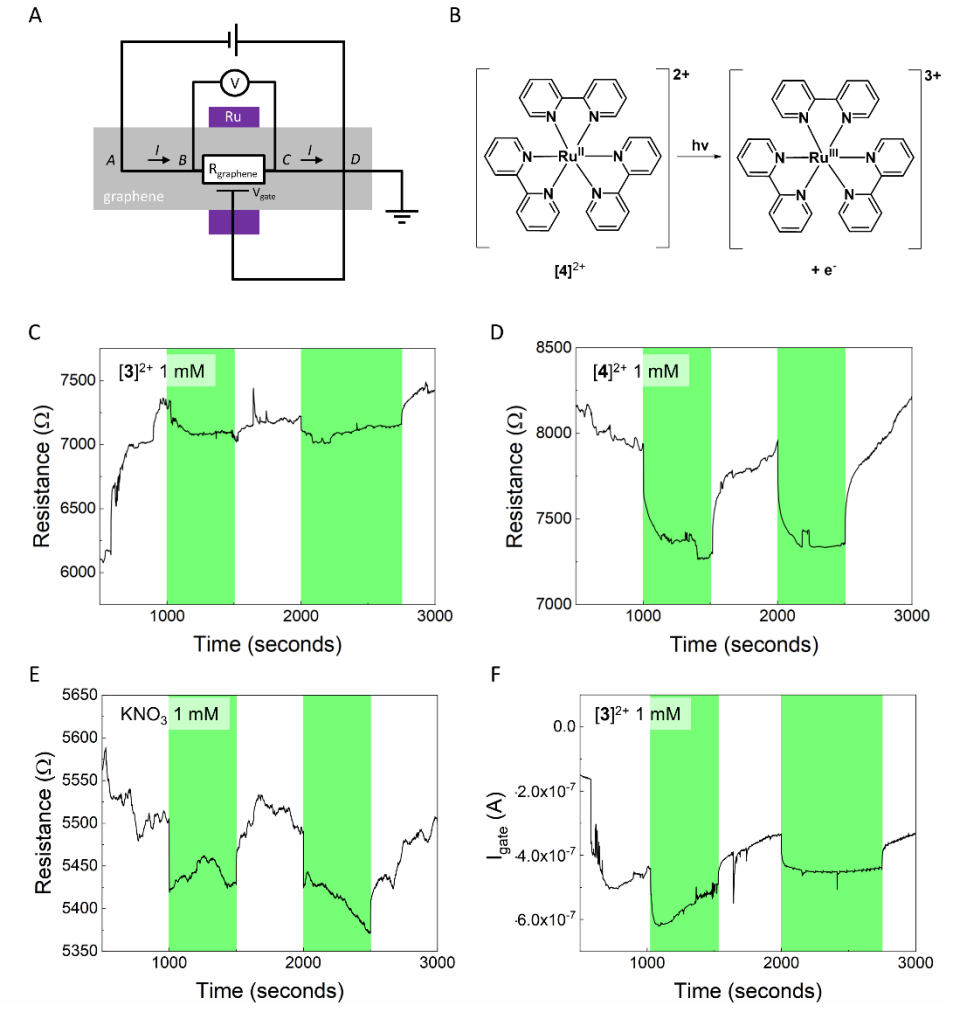

Figure 5.3: Electrical characterization of GFETs on paper: resistance over time. A) Electrical scheme for the four-terminal resistance measurements of graphene on paper devices. Resistance (*R*) was measured between electrodes *B* and *C*, while a potential was applied on *A* and *D*, V_{AD} = 250 mV, V_{gate} = 0 V. B) Reaction scheme for the photo-oxidation of [**4**]$^{2+}$, the electron can be transferred to an electron acceptor. C) *R vs.* time in dark (white regions) and light-irradiated conditions (green regions) for a GFET on paper, soaked with a solution of [**3**]$^{2+}$ (1 mM) in water. D) *R vs.* time in dark (white regions) and light-irradiated conditions (green regions) for a GFET on paper, soaked with a solution of [**4**]$^{2+}$ (1 mM) in water. E) *R vs.* time in dark (white regions) and light-irradiated conditions (green regions) for a GFET on paper, soaked with a solution of KNO_3 (1 mM) in water. F) I_{gate} *vs.* time for the same GFET as in C. Green boxes indicate when devices were irradiated with green light (530 nm, *P* = 8.15 mW).

Interestingly, independently from the chemical nature of the additive in the soaking solution, the GFETs on paper showed the same response to green light irradiation (Figure 5.3C-E): when the irradiation was turned on, *R* between

electrodes *B* and *C* suddenly dropped, while when light was turned off, the resistance abruptly increased. *R vs.* time was in fact quite unstable, yet the current from the gate electrode to the graphene sheet I_{gate}, or leak current, was more stable than *R vs*. time and also dropped abruptly when the device was irradiated and increased abruptly when light was turned off (Figure 5.3F for **[3]**$^{2+}$ and Figure S5.2 for **[4]**$^{2+}$ and KNO_3). However, the behavior of I_{gate} *vs.* time was also independent from the chemical composition of the solution. The presence of the complex **[3]**$^{2+}$ in the device wetting solutions was thus not directly responsible for the resistance or leak current variations of the devices to green light, and further study was required to examine the role of ruthenium in the solutions.

5.2.3. Electrical gating of Ru-soaked devices

To further investigate the effect of green light irradiation on GFETs on paper, in presence of **[3]**$^{2+}$, **[4]**$^{2+}$ or KNO_3, gating experiments were performed to electrically characterize the graphene sheet of the devices. Gating cycles were performed in the dark (state I), during irradiation with green light (state II) and again in the dark (state III). In each state, the gate voltage (V_{gate}) was cycled 5 times between 0 and 1.5 V, while prior to state I, 10 cycles were performed for stabilization. We observed the ambipolar behavior of graphene[15] in *R vs.* V_{gate} in all states (dark-light-dark) for GFETs soaked with either of the solutions containing **[3]**$^{2+}$, **[4]**$^{2+}$ or KNO_3 (all 1 mM): the Dirac point of graphene (a maximum in *R vs.* V_{gate}) was located at V_{gate} = 0.8 V for these devices when sweeping backward (1.5 to 0 V, see Figure 5.4A, C and E). Notably, in forward sweeps *R vs.* V_{gate} typically was less constant, *i.e.* the differences between separate gating cycles were larger than in the backward sweeps (see Figure S5.3). While for **[3]**$^{2+}$ the difference between forward and backward sweeps was not very large (Figure S5.3A and B), we found that for **[4]**$^{2+}$ R_{max} in the forward sweep was always much higher (up to 130 kΩ) than during the backward sweep (R_{max} ≤ 28 kΩ, Figure S5.3C and D), which was also the case for KNO_3 (Figure S5.3E and F, R_{max} ≤ 70 kΩ and 40 kΩ for the forward and backward sweeps, respectively). In fact, for **[4]**$^{2+}$ we found that R_{max} varied between sweeps, most strongly in the forward sweeps, but also in the backward sweeps. We believe the large differences in R_{max} between the forward and backward sweeps were due to electrochemical processes occurring during the forward sweep, in the same V_{gate} range (0.5 - 1.0 V) as the Dirac point was located, indicated by the peaks in I_{gate} *vs.* V_{gate} at V_{gate} = 0.7 V during the forward sweeps (see Figure 5.4B, D and F), possibly from an oxidation reaction.

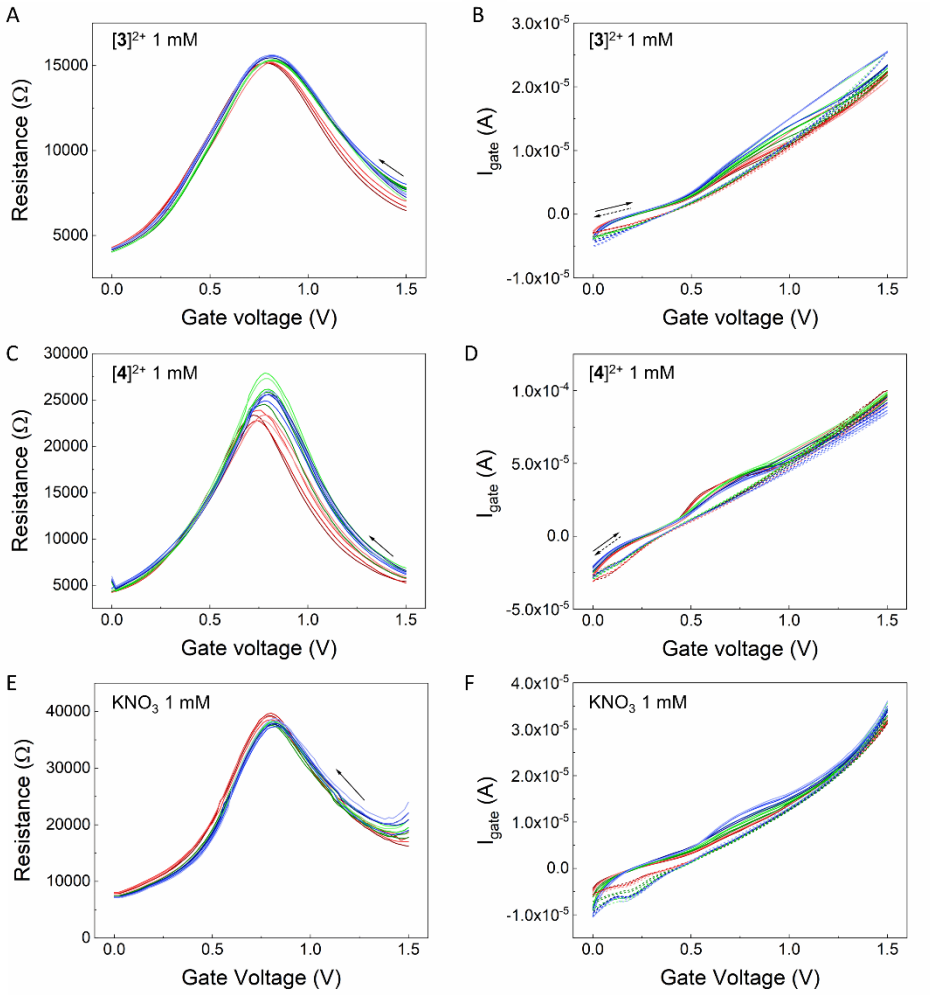

Figure 5.4: Electrical characterization of GFETs on paper: gate sweeping. Resistance *R* and leak current I_{gate} *vs.* V_{gate} for devices wetted with **[1]**Cl, hydrolyzed into $[\mathbf{3}]^{2+}$ (1mM, A-B), $[\mathbf{4}]^{2+}$ (1 mM, C-D), or KNO_3 only (1 M, E-F). A, C and E show the backward sweeps of *R vs.* V_{gate}, while B, D, F, show I_{gate} *vs.* V_{gate}. Starting in the dark (state I, red lines), a typical device was irradiated with green light (state II, green lines), then put back to dark conditions (state III, blue lines). After 10 dark stabilization cycles, 5 V_{gate} cycles were recorded for each state between 0 and 1.5 V which are shown as their corresponding dark to light colors (dark to light red for state I, etc.), solid/dashed line indicates forward/backward sweep, varied at 0.02 Vs^{-1}. *R* was measured between electrodes *B* and *C*, while a potential was applied on *A* and *D*, V_{AD} = 250 mV. Devices were irradiated with green light (530 nm, *P* = 8.15 mW).

In the backward sweep, we could not observe peaks in the leak current in the V_{gate} range of the Dirac point (1.0 – 0.5 V), albeit a reduction peak appeared at 0.2 V for $[\mathbf{4}]^{2+}$ and KNO_3, and we think that electrochemical processes did not influence the *R vs.* V_{gate} profiles. Therefore, we mainly considered the backward sweeps for

comparison between devices, which did not show notable changes in the Dirac point for devices soaked with solutions of [**3**]$^{2+}$, [**4**]$^{2+}$ or KNO_3 (Figure 5.4A, C and E). The Dirac point of the graphene sheet in GFETs on paper soaked with these solutions did thus not change as a result of irradiation, but R_{max} could change, possibly due to electrochemical processes.

5.2.4. Monitoring a photoreaction with graphene on paper

After the electronic characterization of the GFETs on paper, we wanted to investigate if we could use these GFETs to monitor the coordination reaction of dGMP to [**3**]$^{2+}$, forming [**2**]$^{2+}$ in the dark, as well as the reverse photosubstitution reaction upon irradiation. Devices that were soaked with a solution of [**3**]$^{2+}$ and dGMP that was kept in the dark overnight prior to use to allow the formation of [**2**]$^{2+}$, were irradiated with green light (530 nm, P = 8.15 mW, irradiation periods of 500 s) to trigger the release of dGMP from complex [**2**]$^{2+}$ while the resistance of the graphene sheet was monitored over time. We assumed that the opacity of the paper would not be problematic for the photoreaction as the graphene sheet only feels the molecules that react close to the graphene-paper interface, where the light is most intense (as graphene and PMMA are transparent, the light will travel unhindered until it reaches the graphene-paper interface, see Figure 5.5A). Here, R *vs.* time and I_{gate} *vs.* time both responded to irradiation with an abrupt decrease and increase when irradiation was turned on and off, respectively (Figure 5.5B and Figure S5.2D), similar to devices that were wetted with either [**3**]$^{2+}$, [**4**]$^{2+}$, or KNO_3 (all 1 mM). Thus, when we consider R and I_{gate} *vs.* time, we cannot convincingly monitor the conversion of [**2**]$^{2+}$ to [**3**]$^{2+}$ and dGMP under irradiation, or vice versa (in the dark).

We turned again to the gating experiments to further study the light effect on GFETs wetted with [**3**]$^{2+}$ and dGMP (both 1 mM). Interestingly, in the backward sweeps R *vs.* V_{gate} did not remain constant but showed a Dirac peak shift to less positive values upon irradiation (Figure 5.5C), unlike what we observed for GFETs on paper wetted with [**3**]$^{2+}$, [**4**]$^{2+}$, or KNO_3 (all 1 mM). This peak shift appeared to be reversible; in the dark after irradiation (state III), the Dirac peak shifted to more positive values again. In the backward sweep, we only observed a peak in I_{gate} *vs.* V_{gate} at 0.2 V, far away from the Dirac point in the backward sweep (Figure 5.5D), so electrochemistry did not seem to affect the R *vs.* V_{gate} plots during the backward sweep. In the forward sweeps, we found in fact two peaks in I_{gate} *vs.*

V_{gate} at 0.6 and 1.3 V, indicative of two different electrochemical reactions taking place, possibly because two ruthenium species were present in solution, *i.e.* $[\mathbf{2}]^{2+}$ and $[\mathbf{3}]^{2+}$. Moreover, R_{max} increased in the forwards sweep as more gate cycles were performed (Figure S5.4A and B), similar to what we observed for $[\mathbf{4}]^{2+}$ and KNO_3, possibly due to similar electrical processes. Overall, the negative Dirac point shift in the backward sweeps of GFETs wetted with $[\mathbf{3}]^{2+}$ and dGMP could be the result of the light-driven dissociation of dGMP from $[\mathbf{2}]^{2+}$ taking place, but it is hard to conclude, as the Dirac peak shift is rather small, and other electrochemical processses appear to be involved as well.

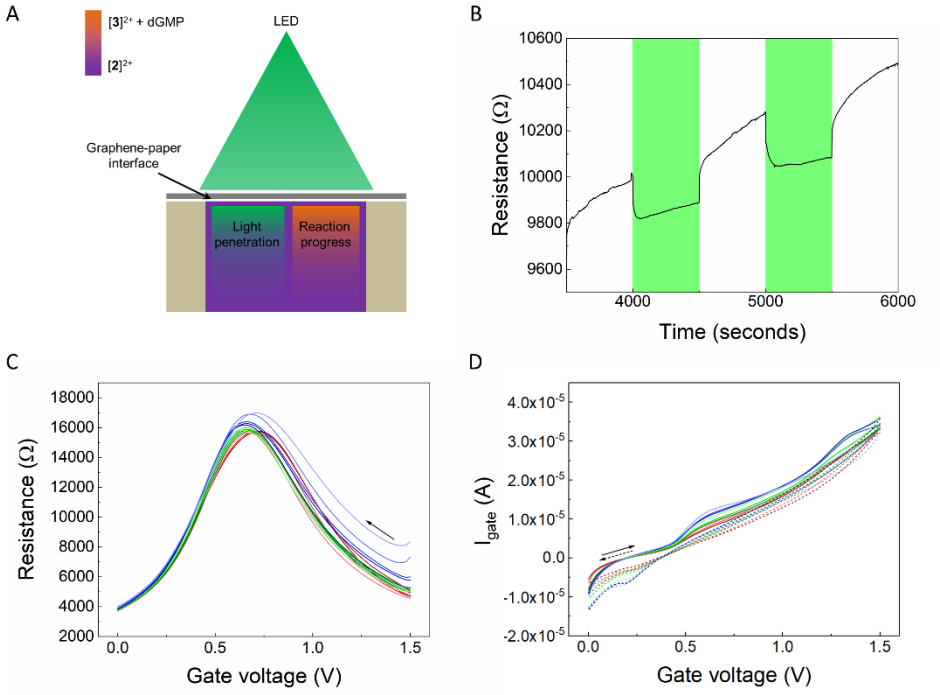

Figure 5.5: Light response of a GFET device wetted with a solution of $[3]^{2+}$ (1mM) + dGMP (1 mM). A) Schematic of green light penetration and reaction progress at the graphene-paper interface. The PMMA layer on top of graphene is not shown here, as it is fully transparent and does not interfere with irradiation. B) *R vs.* time in dark (white regions) and light-irradiated conditions (green regions) for a GFET on paper, soaked with a solution of $[\mathbf{3}]^{2+}$ (1 mM) + dGMP (1 mM) in water. Green boxes indicate when the device was irradiated with green light (530 nm, P = 8.15 mW). C, D) *R vs.* V_{gate} and I_{gate} *vs.* V_{gate} for devices wetted with $[\mathbf{3}]^{2+}$ (1mM) + dGMP (1 mM) in water. C shows the backward sweep of *R vs.* V_{gate}, while D shows I_{gate} *vs.* V_{gate}. Starting in the dark (state I, red), a typical device was irradiated with green light (state II, green line), back to dark (state III, blue line). After 10 dark stabilization cycles, 5 V_{gate} cycles were recorded for each state between 0 and 1.5 V which are shown as their corresponding dark to light colors (dark to light red for state I, etc.), solid/dashed line indicates forward/backward sweep, varied at 0.02 Vs^{-1}. R was measured between electrodes B and C, while a potential was applied on A and D, V_{AD} = 250 mV.

5.2.5. Photochemistry versus electrochemistry

The electrical behavior of all soaked devices, both in presence and absence of ruthenium complexes, strongly suggested that electrochemical processes occurred near or at the graphene sheet in all cases, possibly modifying the sheet itself. As the modifications in *R vs.* V_{gate} appear to be reversible, the graphene sheet itself seems not to be permanently modified by these processes.[16] We likely observed oxidation (in the forward sweep) and reduction (in the backward sweep) of the ruthenium complexes **[2]**$^{2+}$, **[3]**$^{2+}$ and **[4]**$^{2+}$, as suggested by the peaks in I_{gate} *vs.* V_{gate}. For **[3]**$^{2+}$, I_{leak} *vs.* V_{gate} suggests the complex is being oxidized and reduced again during the gate sweeps. Yet, *R vs.* V_{gate} appears not to be affected by these processes, as the forward and backward sweep overlapped perfectly and *R vs.* V_{gate} did not change over the course of the gating experiment. Therefore, we think that graphene is not actively reacting with complex **[3]**$^{2+}$. In the case of **[4]**$^{2+}$, oxidation from $[Ru^{II}(bpy)_3]^{2+}$ to $[Ru^{III}(bpy)_3]^{3+}$ may lead to an electron transfer process (see Figure 5.3B), with graphene acting as the electron acceptor, similar to an immobilized Ru complex on graphene.[17] The electron transfer may be why we see the large increase of R_{max} in the forward sweep, when the oxidation occurs; as **[4]**$^{2+}$ is oxidized, the current in the graphene sheet is increased, indicated by a peak in the gate current. This gate current appears to play an important role in the high values of R_{max}: due to this second current adding to the circuit, the measurement is likely affected and the measured R values are higher than the actual graphene resistance: the higher the gate current, the higher the resistance (as the residual measurement current in the circuit is lower). For KNO_3, reactions with the copper gate electrode may be involved, as after the gating experiments, occasionally depositions of solid copper appeared to be present on the graphene sheet (see Figure S5.5), which points to the reduction of Cu^{2+} to Cu^0 at the graphene sheet; these Cu^{2+} ions must have been produced by oxidation of the gate copper electrode. Moreover, in *R vs.* V_{gate} we observed an increase in R_{max} in the forwards sweep, which can also be attributed to the oxidation of Cu^0 to Cu^{2+}, with an increase of the gate current in the forward sweep, causing R to be overstated.

It should be noted that the existence of the gate current was present in all devices, and possibly overstated the resistance values in all devices. The Dirac point position was not significantly affected by the leak current though, and can still be used for analysis of the gating experiments.

For the GFETs wetted with $[\mathbf{3}]^{2+}$ + dGMP, it is hard to say what exactly is going on, as multiple processes are occurring at the same time. While multiple species exist in solution, including $[\mathbf{2}]^{2+}$, $[\mathbf{3}]^{2+}$ and dGMP, the ratio between these species is also expected to vary as a result of light irradiation. We saw that the intensity of the peaks in the leak current (Figure 5.5D) indeed varies during the experiment: for example, the peak at 0.2 V in the backward sweep seemed to be higher during and after irradiation than before irradiation. At the same time, we observed a negative Dirac peak shift, which points to the photochemical conversion taking place, which is being sensed by graphene. At this point, due to the complexity of the results, we cannot exclude either the photochemical reaction or the electrochemical processes from the possible reasons of the Dirac point shift we observed.

5.3. Conclusions & Outlook

Graphene field effect transistors were fabricated on paper, which were found to be green-light responsive when they were soaked with solutions of $[\mathbf{3}]^{2+}$, $[\mathbf{4}]^{2+}$, KNO_3, or $[\mathbf{3}]^{2+}$ + dGMP. When the resistance of the devices was monitored as a function of time, in all cases sharp decreases in *R* occurred when irradiation was started, while *R* increased abruptly again when the light was turned off. When the resistance was monitored while at the same time the potential of the gate electrode V_{gate} was varied, we could observe the typical Dirac peak in the *R vs.* V_{gate} profile independent of the solution the GFET on paper was wetted with. As we applied multiple gate potential cycles, switching form dark, to light and back to dark, we found that the Dirac point in the *R vs.* V_{gate} did not change in the backward sweep (1.5 – 0 V) for devices that were wetted with solutions of $[\mathbf{3}]^{2+}$, $[\mathbf{4}]^{2+}$ or KNO_3. In the forwards sweep, R_{max} increased for $[\mathbf{4}]^{2+}$ and KNO_3, which is likely due to an overstatement of the measured *R* due to an increased gate current by electrochemical processes. Consistent for all devices, the leak current I_{gate} showed reduction and oxidation peaks, which seemed to indicate that the graphene sheet was involved in electrochemical processes, *i.e.* reduction and oxidation of the ruthenium complexes for $[\mathbf{3}]^{2+}$ and $[\mathbf{4}]^{2+}$ and of copper originating from the gate electrode for KNO_3. Finally, devices that were wetted with a photoreactive solution containing $[\mathbf{3}]^{2+}$ and the dGMP ligand showed a Dirac point shift to less positive values, possibly due to the photochemical conversion taking place. Yet, due to multiple electrochemical processes of this multi-species solution as indicated by multiple peaks in I_{gate} *vs.* V_{gate}, we could not definitively conclude

that these resistance variations were caused by the photoreaction occurring near the graphene sheet, or due to the electrochemical processes in which the graphene sheet itself may be been involved as well. We believe that these paper-based devices show the power of paper for electronic gating and sensing, and that these concepts advance the field of graphene sensors and flexible electronics.

5.4. Acknowledgements

The ruthenium complex [Ru(tpy)(biq)(Cl)](Cl) was kindly provided by Dr. Lucien Lameijer. Jonathan de Ruiter, Daan van den Bos and Camille Blet are thanked for their experimental contributions and scientific discussions. Prof. Dr. Jan van Ruitenbeek is thanked for scientific discussions.

5.5. References and Notes

[1] D. Neumaier, S. Pindl, M. C. Lemme, *Nat. Mater.* **2019**, *18*, 525.
[2] D. R. Cairns, R. P. Witte, D. K. Sparacin, S. M. Sachsman, D. C. Paine, G. P. Crawford, R. R. Newton, *Appl. Phys. Lett.* **2000**, *76*, 1425.
[3] T.-H. Han, H. Kim, S.-J. Kwon, T.-W. Lee, *Mater. Sci. Eng. R Rep* **2017**, *118*, 1.
[4] M. Sher, R. Zhuang, U. Demirci, W. Asghar, *Expert Rev. Mol. Diagn.* **2017**, *17*, 351.
[5] C. Renault, J. Koehne, A. J. Ricco, R. M. Crooks, *Langmuir* **2014**, *30*, 7030; E. Carrilho, A. W. Martinez, G. M. Whitesides, *Anal. Chem.* **2009**, *81*, 7091; A. W. Martinez, S. T. Phillips, B. J. Wiley, M. Gupta, G. M. Whitesides, *Lab Chip* **2008**, *8*, 2146.
[6] E. Han, J. Yu, E. Annevelink, J. Son, D. A. Kang, K. Watanabe, T. Taniguchi, E. Ertekin, P. Y. Huang, A. M. van der Zande, *Nat. Mater.* **2020**, *19*, 305; C. Lee, X. Wei, J. W. Kysar, J. Hone, *Science* **2008**, *321*, 385.
[7] W. Fu, L. Jiang, E. P. van Geest, L. M. C. Lima, G. F. Schneider, *Adv. Mater.* **2017**, *29*, 1603610.
[8] G. Yang, C. Lee, J. Kim, F. Ren, S. J. Pearton, *Phys. Chem. Chem. Phys.* **2013**, *15*, 1798; S. Kumar, S. Kaushik, R. Pratap, S. Raghavan, *ACS Appl. Mater. Interfaces* **2015**, *7*, 2189.
[9] M. Zhang, C. Hou, A. Halder, H. Wang, Q. Chi, *Mater. Chem. Front.* **2017**, *1*, 37; Z. Weng, Y. Su, D.-W. Wang, F. Li, J. Du, H.-M. Cheng, *Adv. Energy Mater.* **2011**, *1*, 917.
[10] A. Bahreman, B. Limburg, M. A. Siegler, E. Bouwman, S. Bonnet, *Inorg. Chem.* **2013**, *52*, 9456.
[11] H. Chan, J. B. Ghrayche, J. Wei, A. K. Renfrew, *Eur. J. Inorg. Chem.* **2017**, *2017*, 1679.
[12] K. Kalyanasundaram, *Coord. Chem. Rev.* **1982**, *46*, 159.
[13] B. Limburg, E. Bouwman, S. Bonnet, *ACS Catal.* **2016**, *6*, 5273.
[14] K. Kalyanasundaram, J. Kiwi, M. Grätzel, *Helv. Chim. Acta* **1978**, *61*, 2720; M. Kirch, J.-M. Lehn, J.-P. Sauvage, *Helv. Chim. Acta* **1979**, *62*, 1345.
[15] K. S. Novoselov, A. K. Geim, S. V. Morozov, D. Jiang, Y. Zhang, S. V. Dubonos, I. V. Grigorieva, A. A. Firsov, *Science* **2004**, *306*, 666.
[16] V. Georgakilas, M. Otyepka, A. B. Bourlinos, V. Chandra, N. Kim, K. C. Kemp, P. Hobza, R. Zboril, K. S. Kim, *Chem. Rev.* **2012**, *112*, 6156.
[17] X. Liu, E. K. Lee, J. H. Oh, *Small* **2014**, *10*, 3700.